PROCEEDINGS OF SCIENCE

Pseudo- and quasi-PDFs in the BFKL approximation

Giovanni Antonio Chirilli[a,*]

[a] *Institut für Theoretische Physik, Universität Regensburg, Universitätsstrasse 31, D-93040 Regensburg, Germany*

E-mail: giovanni.chirilli@ur.de

To calculate the parton distribution functions (PDF) from first principles using lattice gauge theories it is convenient to consider the Ioffe-time distribution defined through gauge-invariant bi-local operators with spacelike separation. Lattice calculations provide values for a limited range of the distance separating the bi-local operators. In order to perform the Fourier transform and obtain the pseudo- and the quasi-PDFs, it is then necessary to extrapolate the large-distance behavior.

I will discuss the formalism one may use to study the behavior of the Ioffe-time distribution at large distances and show that the pseudo-PDF and quasi-PDF are very different in this regime. Using light-ray operators, I will also show that the higher twist corrections of the quasi-PDF come in not as inverse powers of P but as inverse powers of $x_B P$.

41st International Conference on High Energy physics - ICHEP2022
6-13 July, 2022
Bologna, Italy

*Speaker

PoS(ICHEP2022)826

1. Introduction

The Euclidean formulation of the lattice gauge theory does not allow direct calculations of the parton distribution functions (PDF). So far, the most successful procedure to overcome this difficulty is represented by the study of equal-time correlators in coordinate space called Ioffe-time distributions. Two different Fourier transforms of the Ioffe-time distributions lead to the quasi-PDF [1] and the pseudo-PDF [2].

As originally suggested in ref. [1], to extract the PDF from the quasi-PDF one has to take the infinite-momentum limit $P \to \infty$ with the higher twist corrections are expected to come in as inverse powers of the longitudinal momentum. Using the pseudo-PDFs, instead, the PDFs are extracted in the short (longitudinal) distance limit [2]. Since lattice calculations provide values of the Ioffe-time distributions only for a limited range of the distance separating the bi-local operators, in order to perform the Fourier transform for the quasi-PDF or the pseudo-PDF, one has to extrapolate the large-distance behavior [3].

For the first time, in Ref [4], we obtained the behavior of the gluon Ioffe-time distribution at large longitudinal distances as well as the low-x_B behavior of the quasi-PDF and pseudo-PDF. Using the light-ray operators, obtained as an analytic continuation of local twist-two operators [6, 7], we extracted also the leading twist (LT) and next-to-leading twist (NLT) contributions.

2. Pseudo-PDF and quasi-PDF from Ioffe-time distribution

The pseudo-PDF and the quasi-PDF are obtained from two different Fourier transforms of the Ioffe-time distributions. As we will see, these differences will lead to two completely different behaviors at small-x$_B$. The gluon bi-local operator, $M_{\mu\alpha;\lambda\beta} \equiv \langle P|G_{\mu\alpha}(z)[z,0]G_{\lambda\beta}(0)|P\rangle$, defining the Ioffe-time distribution, can be decomposed in terms of six tensor structures proportional to invariant amplitudes of the type $\mathcal{M}(z^2, P^2)$, using the proton momentum P^μ, the coordinate z^μ and the metric tensor $g^{\mu\nu}$ [8]. The light-cone gluon distribution is determined from $g_\perp^{\alpha\beta} M_{+\alpha;+\beta}(z^+, P)$ with z taken on the light-cone and proportional to the invariant amplitude

$$g_\perp^{\alpha\beta} M_{+\alpha;+\beta}(z^+, P) = 2(P^-)^2 \mathcal{M}_{pp}(z\cdot p, 0)\,. \tag{1}$$

As usual, we define the light-cone coordinates $x^\pm = \frac{x^0 \pm x^3}{\sqrt{2}}$, and light-cone vectors n^μ and n'^μ such that $n\cdot n' = 1$, $n\cdot x = x^-$ and $n'\cdot x = x^+$.

The relation between the gluon PDF $D_g(x_B)$ and the amplitude $\mathcal{M}_{pp}$ is given by

$$\mathcal{M}_{pp}(z\cdot P, 0) = \frac{1}{2}\int_{-1}^{1} dx_B\, e^{iz\cdot P\, x_B}\, x_B D_g(x_B)\,. \tag{2}$$

The gluon Ioffe-time distribution $\mathcal{M}_{pp}(z\cdot P, z^2)$, with $z\cdot P$ the Ioffe-time parameter is given in terms of the zeroth and transverse components as

$$M_{0i;i0} + M_{ji;ij} = 2P_0^2 \mathcal{M}_{pp}\,. \tag{3}$$

Since at high energy (Regge) limit the transverse components are suppressed while the 0th and 3rd components cannot be distinguished, calculating the behavior of the left-hand-side (LHS) of (1), will

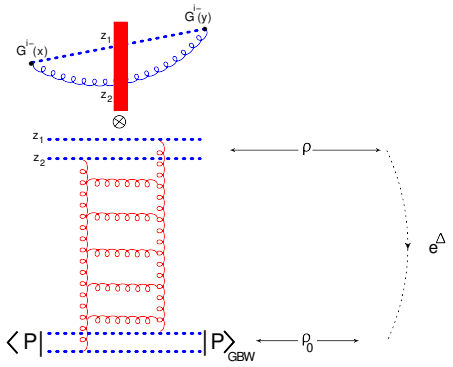

Figure 1: Diagrammatic representation of the HE-OPE applied to the gluon non-local operator with "quasi-PDF frame".

be equivalent, at high-energy, to calculating the behavior of RHS of (3). The momentum-density pseudo-PDF is defined as the Fourier transform with respect to $z \cdot P$, that is a Fourier transform with respect to P keeping its orientation fixed. So, we define the gluon pseudo-PDF as

$$G_{\rm p}(x_B, z^2) = \int \frac{d\varrho}{2\pi}\, e^{-i\varrho\, x_B}\, \mathcal{M}_{pp}(\varrho, z^2)\,, \tag{4}$$

where we defined $\varrho \equiv z \cdot P$. The momentum-density quasi-PDF is defined, instead, as the Fourier transform with respect to z^μ keeping its orientation fixed. Let us define the vector $\xi^\mu = \frac{z^\mu}{|z|}$, the real parameter ς such that $-z^2 = \varsigma^2 > 0$, and $P_\xi = P \cdot \xi$. The quasi-PDF is then defined as

$$G_q(x_B, P_\xi) = P_\xi \int \frac{d\varsigma}{2\pi}\, e^{-i\varsigma\, P_\xi x_B}\, \mathcal{M}_{pp}(\varsigma P_\xi, \varsigma^2)\,. \tag{5}$$

We will calculate the large distance (large ϱ) behavior of the Ioffe-time distribution $\mathcal{M}_{pp}(\varrho, z^2)$, and the low-$x_B$ behavior of the gluon pseudo-PDF (4), and of the gluon quasi-PDF (5).

3. Low-x_B behavior from high-energy OPE

To get the low-x_B behavior of the gluon pseudo- and quasi-PDF we should first consider the behavior of the Ioffe-time distribution for large values of the ϱ parameter using the high-energy operator product expansion (HE-OPE) (see [9] for review).

The Ioffe-time gluon distribution defined in the previous section is

$$\langle P|G^{ai-}(z)[z,0]G_i^{b-}(0)|P\rangle = 2(P^-)^2 \mathcal{M}_{pp}(\varrho, z^2)\,. \tag{6}$$

The HE-OPE procedure requires that one calculates the coefficient function (Impact Factor) first, and then the resummation of the relevant logarithms is obtained through the evolution with respect to the rapidity parameter of the resulting operators. The aforementioned procedure is schematically given in Fig 1 and the result in the saddle point approximation is [4]

$$\mathcal{M}_{pp}(\varrho, z^2) \simeq \frac{3N_c^2}{128\,\varrho}\frac{Q_s\,\sigma_0}{|z|}\left(\frac{2\,\varrho^2}{z^2 M_N^2} + i\epsilon\right)^{\bar\alpha_s 2\ln 2} \frac{e^{-\frac{\ln^2\frac{Q_s|z|}{2}}{7\zeta(3)\bar\alpha_s \ln\left(\frac{2\varrho^2}{z^2M_N^2}+i\epsilon\right)}}}{\sqrt{7\zeta(3)\bar\alpha_s \ln\left(\frac{2\,\varrho^2}{z^2 M_N^2} + i\epsilon\right)}}\,. \tag{7}$$

In eq. (7), the first thing we should notice is that the logarithms resummed by BFKL are $\bar{\alpha}_s \ln\left(\frac{\sqrt{2}\varrho}{|z|M_M}\right)$. The second is that the Ioffe-time ϱ acts like a rapidity parameter. We evolve the distribution in ϱ as long as $\bar{\alpha}_s \ln\left(\frac{\sqrt{2}\varrho}{|z|M_M}\right)$ is of order 1, i.e. we start the evolution at large values of ϱ and end at smaller ones. The dipole at the smallest value of ϱ is evaluated in the GBW model. We stopped the evolution at $\varrho = 10$ (see figure 1).

Considering the case $0 < \frac{Q_s^2|z|^2}{4} < 1$, which corresponds to the typical DIS region, taking the first two leading residues, we obtain the twist expansion as [4]

$$\mathcal{M}_{pp}(\varrho, z^2) = \frac{N_c^2}{8\pi^2\bar{\alpha}_s}\frac{Q_s^2\sigma_0}{\varrho}\left(\frac{4\bar{\alpha}_s\left|\ln\frac{Q_s|z|}{2}\right|}{\ln\left(\frac{2\,\varrho^2}{z^2M_N^2}+i\epsilon\right)}\right)^{\frac{1}{2}} I_1(\tilde{t})\left(1+\frac{Q_s^2|z|^2}{5}\right)+O\left(\frac{Q_s^4|z|^4}{16}\right), \tag{8}$$

with $\tilde{t} = \left[4\bar{\alpha}_s\left|\ln\frac{Q_s|z|}{2}\right|\ln\left(\frac{2\,\varrho^2}{z^2M_N^2}+i\epsilon\right)\right]^{\frac{1}{2}}$. Results (7) and (8) are plotted in Fig. 2.

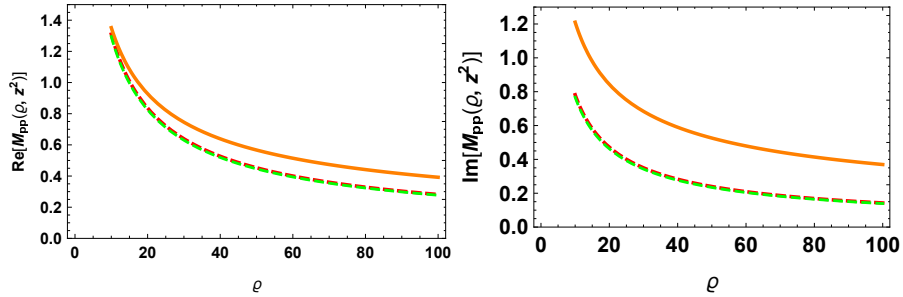

Figure 2: In the left panel, the orange curve is the numerical evaluation of the real part of eq. (7), the green dashed curve is the real part of the LT term only, while the red dashed one is the real part of LT+NLT result (8). In the right panel, we plot the imaginary parts.

3.1 Gluon pseudo- and quasi-PDF with BFKL resummation

The pseudo-PDF is obtained from eq. (4) performing the Fourier transform with respect to ϱ. In the saddle point approximation, the result is

$$\begin{aligned} G_{\rm p}(x_B, z^2) \;&\simeq\; -i\frac{3N_c^2}{128\pi}\frac{Q_s\sigma_0}{|z|}\frac{\Gamma(\bar{\alpha}_s 4\ln 2)\sin(\frac{\pi}{2}\bar{\alpha}_s 4\ln 2)}{\sqrt{7\zeta(3)\bar{\alpha}_s\ln\left(\frac{2}{x_B^2z^2M_N^2}+i\epsilon\right)}}\text{sign}(x_B) \\ &\times\; \exp\left\{\frac{-\ln^2\frac{Q_s|z|}{2}}{7\zeta(3)\bar{\alpha}_s\ln\left(\frac{2}{x_B^2z^2M_N^2}+i\epsilon\right)}\right\}\left(\frac{2}{x_B^2z^2M_N^2}+i\epsilon\right)^{\bar{\alpha}_s 2\ln 2}. \end{aligned} \tag{9}$$

In result (9) one can immediately observe the typical low-x_B resummation of logarithms $\bar{\alpha}_s \ln 1/x_B$ with $\bar{\alpha}_s 2\ln 2$ the famous Pomeron intercept. Similarly, we can perform the Fourier transform (4) in the leading and next-to-leading twist approximation.

$$G_{\rm p}(x_B, z^2) = \frac{N_c^2Q_s^2\sigma_0}{16\pi^3\bar{\alpha}_s}\left(1+Q_s^2|z|^2/5\right)I_0(h)+O\left(Q_s^4|z|^4/16\right), \tag{10}$$

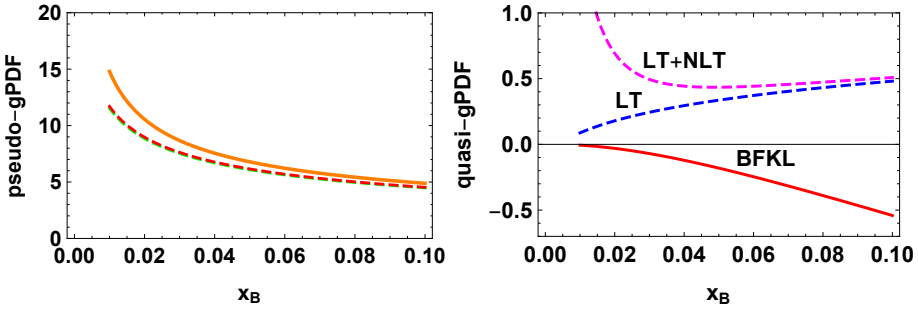

Figure 3: In the left panel we plot the pseudo-PDF with BFKL resummation (orange curve), and the LT (green dashed curve) and LT+NLT (red dashed curve) of the pseudo-PDF result; In the right panel, we plot quasi-PDF with BFKL resummation (real part), the LT, and the LT+NLT (real part). The curves are plotted in the range $x_B \in [0.01, 0.1]$ with $P_\xi = 4\,\text{GeV}$. The value of x_B is between 0.1 to 0.01 in both plots.

with $h = \left[2\bar{\alpha}_s \left|\ln 4/(|z|^2 Q_s^2)\right| \ln 2/(x_B^2 |z^2| M_N^2)\right]^{\frac{1}{2}}$, and I_0 the modified Bessel function. In Fig. 3, we plot the gluon pseudo-PDF with the BFKL resummation eq. (9) (orange curve), and the LT term and the LT plus NLT (green dashed and red dashed curve respectively). We observe that the BFKL resummation result agrees with the LT and LT+NLT result in the region of moderate x_B. When we move into the low-x_B region, we notice a strong disagreement which confirms the necessity of a $\ln \frac{1}{x_B}$ resummation represented by the BFKL equation [10, 11].

For the quasi-PDF case, we need to perform a Fourier transform with respect to a different parameter. The quasi-PDF is defined as the Fourier transform of the coordinate-space gluon distributions keeping, this time, the orientation of the vector z^μ fixed.

In the high-energy limit, where $x^+ \to \infty$ and $x^- \to 0$, we can not distinguish between the zeroth and the third component. We can then rewrite $LP^- = z \cdot P = \varsigma P_\xi$ with $P_\xi \equiv P \cdot \xi = P^-$ because the ξ^μ vector, in the limit we are considering, selects the minus component of the P^μ vector. Moreover, in coordinate space, in the high-energy limit, every field depends only on x^+ and $x_\perp$, so, to restore the x^- components we make the substitution $(x-y)_\perp^2 = \Delta_\perp^2 \to -z^2 = \varsigma^2$. So, using the definition of the gluon quasi-PDF eq. (5), performing the integration over ς (recall that we are using $\gamma = \frac{1}{2} + i\nu$) and then taking the saddle point approximation for the integration over ν, we get

$$G_q(x_B, P_\xi) \simeq -\frac{3N_c^2}{256} Q_s \sigma_0 P_\xi |x_B| \left(-\frac{2P_\xi^2}{M_N^2} + i\epsilon\right)^{\bar{\alpha}_s 2\ln 2} \frac{e^{-\frac{\ln^2 \frac{Q_s}{2P_\xi |x_B|}}{7\bar{\alpha}_s \zeta(3) \ln\left(-\frac{2P_\xi^2}{M_N^2} + i\epsilon\right)}}}{\sqrt{7\zeta(3)\bar{\alpha}_s \ln\left(-\frac{2P_\xi^2}{M_N^2} + i\epsilon\right)}}. \tag{11}$$

We notice that, in the gluon quasi-PDF case, the usual exponentiation of the Pomeron intercept (the LO BFKL eigenvalues $\aleph(\gamma)$), which indicates the resummation of large logarithms of $\frac{1}{x_B}$, is absent. To obtain the leading and next-to-leading twist gluon quasi-PDF we have to perform the Fourier à la quasi-PDF and make the inverse Mellin transform at the end. So, using the quasi-PDF variables ς and P_ξ and performing the integration over ς we get

$$G_{\rm q}(x_B, P_\xi) = -\frac{N_c^2 Q_s^2 \sigma_0}{16\bar{\alpha}_s^2\pi^3}\frac{1}{2\pi i}\int_{1-i\infty}^{1+i\infty} d\omega \left(-\frac{2P_\xi^2}{M_N^2}+i\epsilon\right)^{\frac{\omega}{2}} \left(-\frac{4P_\xi^2 x_B^2}{Q_s^2}+i\epsilon\right)^{\frac{\bar{\alpha}_s}{\omega}} \times \left(\omega + \frac{2\bar{\alpha}_s Q_s^2}{5P_\xi^2 x_B^2} + O\left(\frac{\bar{\alpha}_s}{\omega}\right)\right). \tag{12}$$

where we have used the approximation $\bar{\alpha}_s \ll \omega \ll 1$. Equation (12) is the gluon quasi-PDF up to the next-to-leading twist contribution. What one should notice in the result (12) is the strong enhancement of the NLT term with respect to the LT term due to the $\frac{1}{P_\xi^2 x_B^2}$ factor which increases as x_B decreases.

4. Conclusions

The main conclusion is that the pseudo-PDF and the quasi-PDF have very different behavior at low-x_B. The physical origin of the difference between the two distributions is due to the two different Fourier transforms under which they are defined. Indeed, in the pseudo-PDF case, the scale is the resolution, i.e. the square of the length of the gauge link separating the bi-local operator. On the other hand, in the quasi-PDF case, the scale is the energy, i.e. the momentum of the hadronic target (the nucleon) projected along the direction of the gauge link. Therefore, if on one hand, the pseudo-PDF has the typical behavior of the gluon distribution at low-x_B, on the other hand, the quasi-PDF has a rather unusual low-x_B behavior (see figure 3).

References

[1] X. Ji, Phys. Rev. Lett. **110** (2013), 262002 doi:10.1103/PhysRevLett.110.262002

[2] A. V. Radyushkin, Phys. Rev. D **96** (2017) no.3, 034025 doi:10.1103/PhysRevD.96.034025

[3] V. Braun and D. Müller, Eur. Phys. J. C **55** (2008), 349-361 doi:10.1140/epjc/s10052-008-0608-4 [arXiv:0709.1348 [hep-ph]].

[4] G. A. Chirilli, JHEP **03** (2022), 064 doi:10.1007/JHEP03(2022)064 [arXiv:2111.12709 [hep-ph]].

[5] I. Balitsky, Int. J. Mod. Phys. Conf. Ser. **25** (2014), 1460024 doi:10.1142/S2010194514600246

[6] I. Balitsky, V. Kazakov and E. Sobko, [arXiv:1310.3752 [hep-th]].

[7] I. Balitsky, JHEP **04** (2019), 042 doi:10.1007/JHEP04(2019)042 [arXiv:1812.07044 [hep-th]].

[8] I. Balitsky, W. Morris and A. Radyushkin, Phys. Lett. B **808** (2020), 135621 doi:10.1016/j.physletb.2020.135621 [arXiv:1910.13963 [hep-ph]].

[9] I. Balitsky, doi:10.1142/9789812810458_0030 [arXiv:hep-ph/0101042 [hep-ph]].

[10] E. A. Kuraev, L. N. Lipatov and V. S. Fadin, Sov. Phys. JETP **45** (1977), 199-204

[11] I. I. Balitsky and L. N. Lipatov, Sov. J. Nucl. Phys. **28** (1978), 822-829